

Original Article



Downstream Neighbor of Son Overexpression is Associated With Breast Cancer Progression and a Poor Prognosis

Yufeng Qi , Haodong Wu , Conghui Liu , Danni Zheng , Congzhi Yan , Wenjing Hu , Xiaohua Zhang , Xuanxuan Dai

Department of Thyroid and Breast Surgery, The First Affiliated Hospital of Wenzhou Medical University, Wenzhou, People's Republic of China

OPEN ACCESS

Received: Dec 2, 2021

Revised: Apr 19, 2022

Accepted: Jun 3, 2022

Published online: Jun 13, 2022

Correspondence to

Xuanxuan Dai

Department of Thyroid and Breast Surgery,
The First Affiliated Hospital of Wenzhou
Medical University, Wenzhou 325000, People's
Republic of China.

Email: daoshidaixuanxuan@126.com

Xiaohua Zhang

Department of Thyroid and Breast Surgery,
The First Affiliated Hospital of Wenzhou
Medical University, Wenzhou 325000, People's
Republic of China.

Email: Zhangxiaohua@wmu.edu.cn

© 2022 Korean Breast Cancer Society

This is an Open Access article distributed under the terms of the Creative Commons Attribution Non-Commercial License (<https://creativecommons.org/licenses/by-nc/4.0/>) which permits unrestricted non-commercial use, distribution, and reproduction in any medium, provided the original work is properly cited.

ORCID iDs

Yufeng Qi

<https://orcid.org/0000-0001-5633-9386>

Haodong Wu

<https://orcid.org/0000-0001-6552-222X>

Conghui Liu

<https://orcid.org/0000-0001-9475-1718>

Danni Zheng

<https://orcid.org/0000-0001-5390-0211>

ABSTRACT

Purpose: The incidence rate of breast cancer (BC) has increased annually. Downstream neighbor of son (DONSON) critically affects cell cycle progression and maintains stable genomic properties; however, its relevant effects on BC growth and progression require in-depth investigation.

Methods: DONSON upregulation was validated in public databases. DONSON expression in matched BC and adjacent tissues and cell lines (MDA-MB-231, BT-549, and HS-578T) was determined using quantitative reverse transcription polymerase chain reaction. *In vitro* apoptosis, invasion, migration, and proliferation tests were performed to ascertain the functions of DONSON in BC cell lines. Then, using western blot analysis, the levels of DONSON downstream proteins were determined.


Results: Compared to the control, DONSON was expressed at higher levels in BC tissues and cell lines. DONSON knockdown facilitated apoptosis and limited proliferation, migration, invasion, and S/G2 transition of BC cells *in vitro*. Furthermore, DONSON overexpression promoted BC cell proliferation and inhibited apoptosis *in vitro*. Moreover, DONSON knockdown reduced cyclin A1 and cyclin-dependent kinase 2 levels. Moreover, DONSON knockdown limited the progression of epithelial-mesenchymal transition.

Conclusion: DONSON critically affects BC growth and serves as a possible target and marker for the efficacy of subsequent therapies.

Keywords: Breast Neoplasms; Biomarkers; Cyclin-Dependent Kinases; Epithelial-Mesenchymal Transition

INTRODUCTION

Breast cancer (BC) is the most common cancer among women worldwide. According to statistics from the International Agency for Research on Cancer/World Health Organization, 2,261,419 new patients were diagnosed in 2020, representing 11.7% of all cancers and 24.5% of tumors in women. Moreover, the number of deaths from BC is approximately 684,996, accounting for 6.9% of all tumors and 15.5% of tumors in women [1]. BC is classified into triple-negative (15%), human epidermal growth factor receptor 2 (HER2)-positive (HER2+)

Congzhi Yan 
<https://orcid.org/0000-0002-9373-0015>
Wenjing Hu 
<https://orcid.org/0000-0002-8927-2445>
Xiaohua Zhang 
<https://orcid.org/0000-0003-1981-0225>
Xuanxuan Dai 
<https://orcid.org/0000-0001-6445-5619>

Funding

The Zhejiang Medical and Health Science and Technology Project (2019RC204), National Natural Science Foundation of China (81902692), and Natural Science Foundation of Zhejiang province (GF18H160072) financed this study.

Conflict of Interest

The authors declare that they have no competing interests.

Author Contributions

Conceptualization: Dai X; Data curation: Zheng D; Formal analysis: Yan C; Methodology: Hu W; Software: Liu C; Supervision: Zhang X; Writing - original draft: Qi Y; Writing - review & editing: Wu H.

(15%–20%), and hormone receptor (HR)-positive (HR+)/HER2-negative (HER2-) (70%) subtypes based on HER2 and HR status [2]. Although early diagnosis and novel therapeutic drugs, such as HER2-targeted agents and cyclin-dependent kinase (CDK) 4/6 inhibitors, have been developed recently and resulted in prolonged survival, the clinical outcome of patients with advanced BC, which can result in distant metastasis of cancer cells and multiple organ lesions, has only modestly improved, with a 5-year survival rate of < 40% [3-5]. Drug resistance leads to continuous tumor progression, including invasion and metastasis. Continuous invasion and metastasis of cancer to other parts of the body result in patient death [6]. Thus, BC occurrence and development mechanisms must be studied, and a biomarker for sensitivity to current therapy and long-term survival is needed.

A total of 23 pairs of RNA sequencing data from BC and adjacent tissues were analyzed to identify novel markers. Downstream neighbor of son (DONSON), a protein-coding gene located on chromosome 21q60, that is, C2TA or C21orf60, was found to be significantly upregulated in BC tissues compared to adjacent tissues. Regarding its role in cancer, Klümper et al. [7] found that DONSON overexpression is related to the prognosis of patients with renal cell carcinoma (RCC) by performing a The Cancer Genome Atlas (TCGA) database analysis. Moreover, DONSON is critical for cell cycle progression and maintenance of genomic stability in prostate carcinoma according to TCGA and Gene Expression Omnibus (GEO) analysis [8]. Nevertheless, a system-based analysis of biologically relevant DONSON functions in BC is required.

This study verified increased DONSON expression in BC tissues and cell lines. Moreover, high DONSON expression was positively correlated with lymph node metastasis (LNM) and poor prognosis. The biological function of DONSON in the BC cell line was determined by performing loss-of-function tests, and an association between the cell cycle and DONSON expression was suggested. Therefore, as revealed by the findings of the present study, DONSON may play a role in promoting BC progression and may serve as a target for subsequent BC therapies.

METHODS

Validated sample

A total of 48 matched pairs of representative BC and adjacent tissues were collected from the Department of Thyroid and Breast Surgery of The First Affiliated Hospital of Wenzhou Medical University (Wenzhou, China). The respective samples underwent the first snap-freezing process in liquid nitrogen after the surgeon excised the tumor and were then stored at -80°C until analysis. The pathologists performed histological analysis of the respective tissues as directors. Before tissue collection, informed consent was obtained from each patient.

Bioinformatics

Public microarray datasets (GSE38959 and GSE22820) in the GEO (<https://www.ncbi.nlm.nih.gov/mesh/>) and TCGA BC databases (<https://portal.gdc.cancer.gov/>) containing clinically relevant data and gene expression levels of 1,104 primary BC samples and 113 common breast tissues were downloaded. Using the Kaplan-Meier plotter (<https://kmplot.com/analysis/index.php?p=service/mesh/>) and Gene Expression Profiling Interactive Analysis (GEPIA2) (<http://gepia2.cancer-pku.cn/>), this study retrieved information on the survival of patients with BC [9]. Nomogram models were established using multivariate analysis. Time-

dependent receiver operating characteristic curves were used to compare the survival factors. The area under the curve (AUC) was obtained using the “pROC” package in R (R Foundation, Vienna, Austria). Using the single gene set enrichment analysis (GSEA) software (GSEA v3.0, <http://www.broadinstitute.org/gsea>), this study conducted an analysis of cohorts with high and low DONSON expression within TCGA [10]. Using the Tumor IMMune Estimation Resource (TIMER) (<https://cistrome.shinyapps.io/timer/>), this study explored correlations between DONSON and CDK2 in triple-negative BC (TNBC) [11].

Cell culture and transfection

A common breast cell line (MCF-10A) and human BC cell lines (HS-578T, BT-549, MCF-7, and MDA-MB-231) was used in the experimental study. The cell lines were provided by the Cell Bank of the Shanghai Chinese Academy of Sciences (Shanghai, China). The HS-578T, MCF-7, and MDA-MB-231 cell lines were cultured in DMEM (Gibco, Invitrogen, Carlsbad, USA) containing 10% fetal bovine serum (Gibco). Roswell Park Memorial Institute-1640 medium (Gibco, Grand Island, USA) supplemented with 10% fetal bovine serum was used to culture the HS-578T cells. MCF-10A cells were cultured in DMEM-F12 (Gibco) containing 10% fetal bovine serum. All cell lines were cultured in 1% penicillin/streptomycin (Solarbio, Beijing, China) at 37°C with 5% CO₂.

Transfected cells (MDA-MB-231 and BT-549) were seeded in 6-well culture plates at a density of 500,000 cells/well. This study used the small interfering RNAs (siRNAs) developed by Gene Pharma (Shanghai, China) to silence DONSON expression. After premixing the siRNA with Lipofectamine RNAiMAX (Invitrogen, Grand Island, USA) (siRNA:iMAX = 10 μL/4 μL; 100 nM final concentration per well), siRNA was introduced into the cells. The medium was changed 7 hours after transfection, and experiments were performed 48 hours after transfection. The siRNA sequences targeting DONSON included siRNA1-sense: GGAAGAAGCUCAAGGUCUUTT/antisense: AAGACCUUGAGCUUCUUCCTT and siRNA2-sense: CCAACAACUCGAGGUUUAATT/antisense: UUAACCUCGAGUUGUUGGTT. The full-length DONSON sequence was cloned into the expression vector pCMV (GeneChem, Montreal, Canada) to overexpress DONSON. DONSON-pCMV was transfected into HS-578T cells using Lipofectamine 3000 (Invitrogen). After 48 hours, the transfected cells were collected for further analysis.

RNA isolation and quantitative real-time polymerase chain reaction

Total RNA was extracted from the cells and tissues using TRIzol reagent (Thermo Fisher Scientific, Waltham, USA) according to the manufacturer's instructions. Reverse transcription was performed using ReverTra Ace qPCR RT (Toyobo, Osaka, Japan) with a temperature cycling program of 16°C for 5 minutes, 42°C for 30 minutes, and 98°C for 5 minutes. The mRNA expression level was determined by quantitative reverse transcription polymerase chain reaction (qRT-PCR) with a SYBR Premix Ex Taq II kit (RR820A; TaKaRa, Dalian, China). qRT-PCR was performed using the ABI 7500 Real-Time PCR System (Thermo Fisher Scientific) under the following cycling conditions: 95°C for 30 seconds, followed by 40 cycles of 95°C for 5 seconds and 60°C for 34 seconds. This study adopted the 2^{-ΔΔCt} method to analyze the expression levels. The overall experimental process was conducted at least 3 independent times. The following specific primer sequences were used: DONSON-forward, TCCAGCATTGTAGGGCAACAGAAG; and DONSON-reverse, GACAAAGCAGGGTGGAGCCAATAG.

Cell Counting Kit-8 (CCK-8) and colony formation assays

Transfected cells were collected 48 hours after culture. BC cells (2,000 cells per well of MDA-MB-231, 1,500 cells per well of BT-549, and 2,000 cells per well of HS-578T) were seeded in 96-well plates. Cell proliferation was measured using the CCK-8 (Beyotime Biotechnology, Shanghai, China) every 24 hours. Cells were incubated for 3 hours at 37°C, and the absorbance of the solution was measured at 450 nm using a SpectraMax iD3 spectrophotometer (Molecular Devices, San Jose, USA). Moreover, 1,000 cells were seeded evenly in each well of a 6-well plate. After 7 days of culture, colonies were photographed with a camera, counted after fixation with 4% paraformaldehyde, and stained with a crystal violet staining solution for 15 minutes at room temperature. The experimental processes were repeated 3 times.

EdU incorporation assay

The transfected cells were incubated with 10 μ M EDU (Beyotime Biotechnology) for 2 hours, fixed with 4% paraformaldehyde at room temperature for 15 minutes, permeabilized with 0.5% TritonX-100, and stained with 500 μ L click solution at room temperature for 30 minutes. The excess dye was removed by washing with phosphate-buffered saline (PBS), and the cells were counterstained with 4',6-diamidino-2-phenylindole and observed under a fluorescence microscope (Carl Zeiss AG, Oberkochen, Germany). The experimental processes were repeated 3 times.

Transwell migration and invasion assays

Cells were collected and plated onto the upper surface of Transwell inserts (#3422; Corning, New York, USA) (3×10^4 MDA-MB-231, BT-549, and HS-578T cells per well) in serum-free medium. The lower chamber contained 600 μ L of culture medium supplemented with 10% FBS. After 24 hours, the cells on the upper surfaces of the Transwell chamber were removed using cotton swabs. Then, cells on the lower surface were fixed with paraformaldehyde and stained with crystal violet. Finally, positively stained cells in 5 random fields for each experimental condition were counted under a microscope at 20 \times magnification. Using a Matrigel invasion chamber (#354,480; Corning BioCoat, New York, USA), an invasion assay was conducted using the same protocol. The experimental processes were repeated 3 times.

Wound-healing migration assay

The cell migration ability was assessed using a wound healing assay. The transfected cells were seeded into 6-well plates and allowed to grow to 80%–90% confluence. Then, a linear scratch wound was made on the cell monolayer using a sterile 10- μ L pipette tip. After rinsing the wells with PBS to remove unbound cells, the cells were cultured in serum-free medium for 24 hours. Wound healing was monitored by capturing images using an inverted microscope connected to an imaging system (Leica Biosystems GmbH, Wetzlar, Germany) at 0 and 24 hours to measure the migration of cells to the wound area. The experimental processes were repeated 3 times.

Apoptosis assay

The annexin V-FITC apoptosis detection kit (#556,547; BD Biosciences, Franklin Lakes, USA) and flow cytometry were employed to detect apoptosis. The cells were harvested and resuspended in 500 μ L of 1 \times binding buffer. Then, the cells were stained for 5 minutes in the dark with 5 μ L propidium iodide (PI) and for 15 minutes with 5 μ L of Annexin V-FITC. The mean fluorescence of 20,000 cells/sample was determined by flow cytometry (BD Biosciences). The results were analyzed using FlowJo software (FlowJo, Ashland, USA). The

total proportion of apoptotic cells was calculated by adding the proportions of early (Q3, Annexin V+/PI-) and late (Q2, Annexin V+/PI+) apoptotic cells. The experimental processes were repeated 3 times.

Determination of caspase 3 activity

Transfected cells were collected 48 hours after culture. The cells were resuspended and lysed with 100 μ L of precooled lysis buffer for 10 minutes on ice; then, the mixture was centrifuged for 1 minutes. The supernatant was immediately transferred to a fresh tube. The reaction system was subsequently configured as specified in the caspase 3 binding assay kit and maintained at 37°C for 2 hours. The absorbance was measured at 405 nm using a SpectraMax iD3 spectrophotometer (Molecular Devices, Shanghai, China). The experimental processes were repeated 3 times.

Cell cycle assays

Before transfection, cells were serum-starved for 48 hours, rinsed with PBS, and fixed with 70% ice-cold ethanol at -20°C overnight. Subsequently, fixed cells were treated with 0.5 mL of PI/RNase Staining Buffer (BD Biosciences, San Diego, CA, USA) and then incubated for 30 minutes in the dark. Samples were analyzed using the FACSCalibur flow cytometer and FlowJo 7.6 software (FlowJo). The experimental processes were repeated 3 times.

Western blot analysis

Total protein was extracted from cultured cells using RIPA buffer (Solarbio) containing phenylmethanesulfonyl fluoride (Solarbio) for 30 minutes on ice, followed by 1 minute of ultrasonication. After centrifugation at 10,000 rpm for 20 min at 4°C to remove debris, the protein concentration was determined using the bicinchoninic acid assay (Thermo Fisher Scientific). All samples were mixed with the loading buffer and subjected to 10% sodium dodecyl sulfate-polyacrylamide gel electrophoresis (Bio-Rad, Hercules, USA). Then, proteins were transferred to polyvinylidene difluoride membranes (0.45 μ m; EMD Millipore, Billerica, USA) at 300 mA for 2 hours. Membranes were incubated with primary antibodies overnight at 4°C after blocking with 5% fat-free milk. Membranes were washed with PBS and incubated with the corresponding secondary antibodies (1:5,000; Abcam, Cambridge, United Kingdom) at ambient temperature for 1 hour. Then, chemiluminescence was used to visualize the labeled protein bands (Thermo Fisher Scientific). Cytoplasmic protein expression levels were normalized to β -actin using ImageJ software (National Institutes of Health, Bethesda, USA). The experimental process was repeated no less than 3 times independently. The primary antibodies applied in the present study included DONSON (1:500, AV45862; Affinity, Shanghai, China), E-cadherin (1:5,000, 20874-1-AP; Proteintech, Wuhan, China), N-cadherin (1:2,000, 22018-1-AP; Proteintech), vimentin (1:1,000, 5741S; Cell Signaling Technology, Danvers, USA), β -actin (1:5,000, 60008-1-Ig; Proteintech), cyclin A1 (1:500, AF0143; Affinity), CDK2 (1:1,000, 10122-1-AP; Proteintech), Bax (1:5,000, 50599-2-IG; Proteintech), and Bcl-2 (1:2,000, ab182858; Abcam).

Statistical analysis

Statistical analyses were performed using GraphPad Prism 8 software (GraphPad, San Diego, USA) and SPSS version 22.0 (IBM SPSS Inc., Chicago, USA). Pearson's χ^2 test was used to compare categorical variables. For numerical data, 2 groups with a normal distribution were analyzed using Student's *t*-test. Non-normally distributed data were compared using nonparametric statistical tests (Mann-Whitney test for unpaired data and Wilcoxon rank-sum test for paired data). Data are reported as mean \pm standard deviation for continuous variables and frequencies for categorical variables. A *p*-value < 0.05 was considered significant.

Ethical approval and consent to participate

The Ethics Committee of The First Affiliated Hospital of Wenzhou Medical University issued ethical approval, and all individual participants included in this study provided informed consent (approval number: 33665786). This study was conducted in accordance with the principles of the Declaration of Helsinki.

RESULTS

DONSON is overexpressed in BC and associated with a poor prognosis

Datasets were analyzed using GEPIA2 and Kaplan-Meier plotter to examine the association between DONSON expression and prognosis of patients with BC. A correlation was observed between high tumor expression of DONSON and worse prognosis in patients with BC (Figure 1A-C), suggesting that DONSON may function as an oncogene. RNA sequencing was performed on 23 pairs of BC tissues and matching adjacent tissues to examine DONSON expression (Figure 1D). To verify the RNA sequencing results for DONSON, the GEO and TCGA databases were analyzed to determine the gene expression data in BC. GSE22820, a dataset aimed at investigating the clinical relevance of genes, was generated from 176 patients with primary BC and 10 normal breast samples [12]. GSE38959, a dataset aimed at identifying novel molecular targets for TNBC, was obtained from 30 TNBC and 13 normal mammary ductal cells [13]. Figure 1E and F present the DONSON mRNA levels in BC and normal breast tissues within the GEO database (GSE22820, $p < 0.01$; GSE38959, $p < 0.001$). DONSON was expressed at higher levels in 1,104 primary BC tissues than in 113 normal breast tissues from TCGA database ($p < 0.0001$, Figure 1G). qRT-PCR analysis confirmed that DONSON expression was upregulated in tumor tissues compared to adjacent tissues (Figure 1H) and BC cell lines compared to MCF-10A cells (Figure 1I). To better predict the prognosis of patients with BC, a prognostic nomogram was developed (Figure 1J). The nomogram was used to

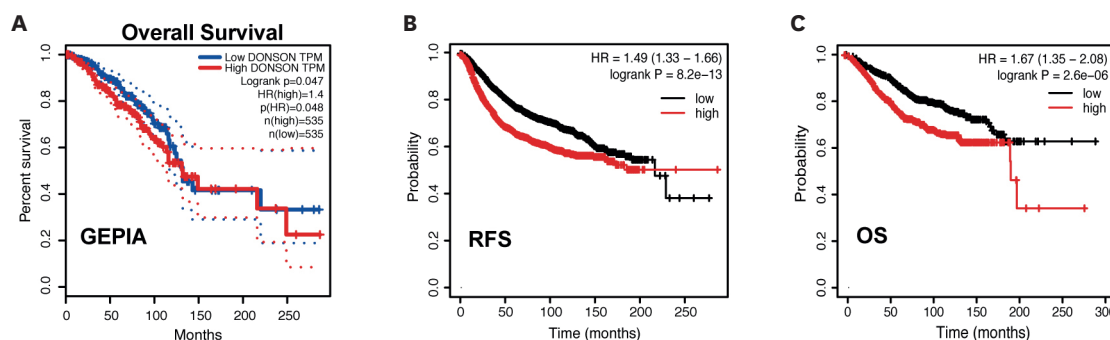


Figure 1. DONSON expression is increased in BC tissues and associated with poor prognosis. (A-C) Correlation between DONSON expression in BC tissues and patient prognosis analyzed using GEPIA2 and Kaplan-Meier plotter. (D) DONSON expression levels in 23 BC tissues compared to matching adjacent tissues from our RNA sequencing dataset. (E, F) DONSON mRNA levels were detected in BC tissues and normal breast tissues in GSE22820 and GSE38959. (G) Correlation of DONSON expression levels in BC tissue and common tissues from TCGA. (H) qRT-PCR analysis of DONSON expression in BC and adjacent tissues ($n = 48$ tissues from each group). (I) qRT-PCR analysis of DONSON expression in BC cell lines. (J) Nomogram by multivariate Cox regression analysis for predicting the proportion of patients with OS. (K) Plots depict the calibration of model in terms of agreement between predicted and observed OS. Model performance is shown by the plot, relative to the 45° line, which represents perfect prediction. (L) AUC plotted for different durations of OS for nomogram-based signature. The statistical analysis used in each panel was as follows: (E-G) Mann-Whitney test, (D, H) Wilcoxon test, and (I) t -test. Images shown are representative of 3 separate experiments.

DONSON = downstream neighbor of son; BC = breast cancer; GEPIA2 = Gene Expression Profiling Interactive Analysis; TCGA = The Cancer Genome Atlas; qRT-PCR = quantitative reverse transcription polymerase chain reaction; OS = overall survival; AUC = area under the curve; RFS = recurrence-free survival; HR = hazard ratio. * $p < 0.05$; † $p < 0.01$; ‡ $p < 0.001$; § $p < 0.0001$.

(continued to the next page)

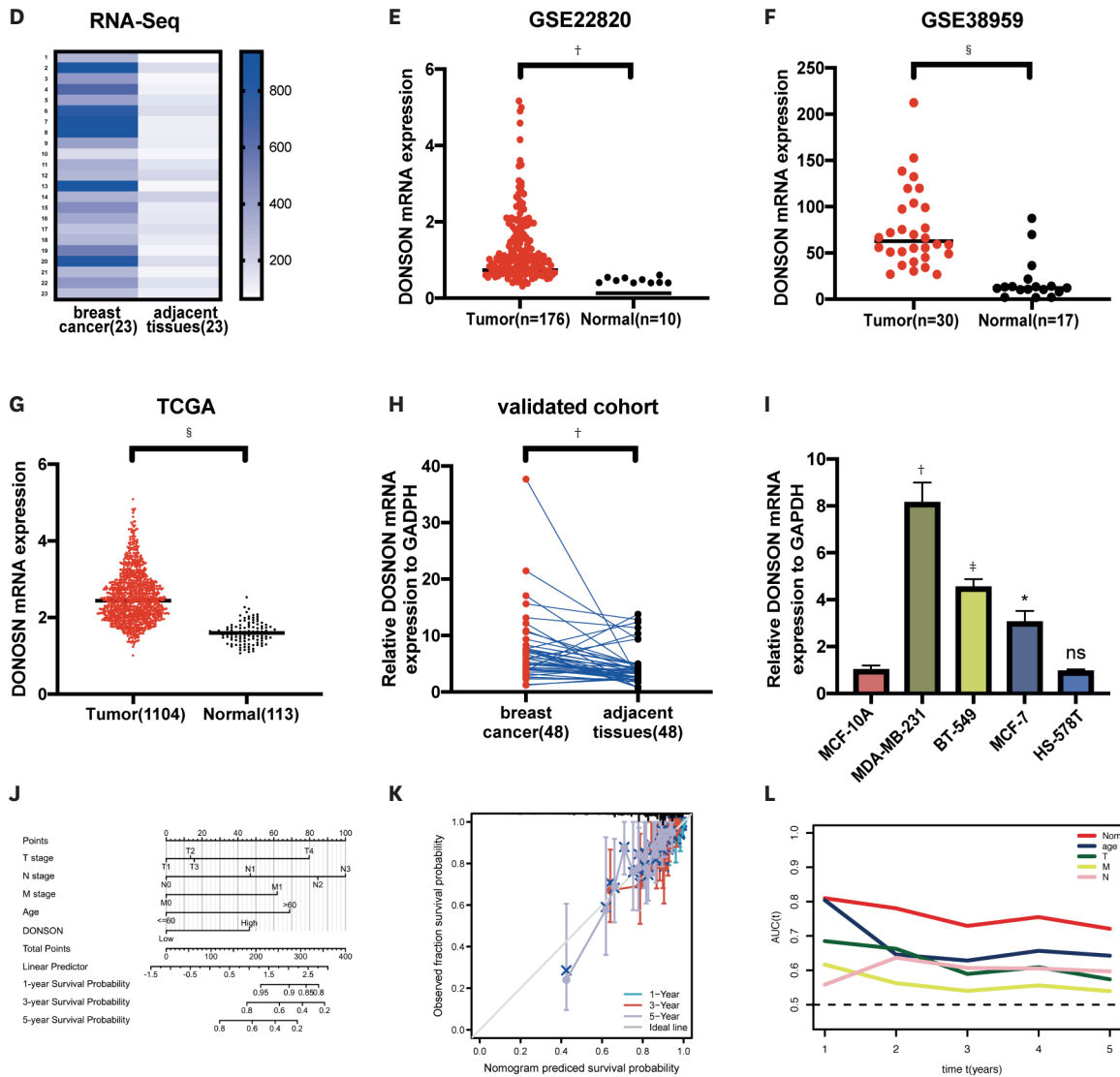


Figure 1. (Continued) DONSON expression is increased in BC tissues and associated with poor prognosis. (A-C) Correlation between DONSON expression in BC tissues and patient prognosis analyzed using GEPIA2 and Kaplan-Meier plotter. (D) DONSON expression levels in 23 BC tissues compared to matching adjacent tissues from our RNA sequencing dataset. (E, F) DONSON mRNA levels were detected in BC tissues and normal breast tissues in GSE22820 and GSE38959. (G) Correlation of DONSON expression levels in BC tissue and common tissues from TCGA. (H) qRT-PCR analysis of DONSON expression in BC and adjacent tissues (n = 48 tissues from each group). (I) qRT-PCR analysis of DONSON expression in BC cell lines. (J) Nomogram by multivariate Cox regression analysis for predicting the proportion of patients with OS. (K) Plots depict the calibration of model in terms of agreement between predicted and observed OS. Model performance is shown by the plot, relative to the 45° line, which represents perfect prediction. (L) AUC plotted for different durations of OS for nomogram-based signature. The statistical analysis used in each panel was as follows: (E-G) Mann-Whitney test, (D, H) Wilcoxon test, and (I) *t*-test. Images shown are representative of 3 separate experiments.

DONSON = downstream neighbor of son; BC = breast cancer; GEPIA2 = Gene Expression Profiling Interactive Analysis; TCGA = The Cancer Genome Atlas; qRT-PCR = quantitative reverse transcription polymerase chain reaction; OS = overall survival; AUC = area under the curve; RFS = recurrence-free survival; HR = hazard ratio. **p* < 0.05; †*p* < 0.01; ‡*p* < 0.001; §*p* < 0.0001.

predict 1-, 3-, and 5-year overall survival (OS) outcomes in individual patients. According to the calibration plot, the nomogram exhibited better performance in predicting the OS of patients (**Figure 1K**). With regard to OS prediction, the nomogram concordance index was 0.724 in TCGA cohorts. Among the factors evaluated in TCGA data, the AUC values revealed that the nomogram was the best predictor of OS (**Figure 1L**). Thus, DONSON is an oncogene associated with BC in public databases.

Table 1. Correlation between DONSON expression and clinicopathologic factors in the TCGA cohort

Features	Patients	High expression	Low expression	Pearson χ^2	p
Sex				1.341	0.247
Women	1,089	543 (98.5)	546 (99.3)		
Men	12	8 (1.5)	4 (0.7)		
Age (yr)				0.392	0.531
< 50	303	147 (26.7)	156 (28.4)		
≥ 50	798	404 (73.3)	394 (71.6)		
Tumor size (mm)				10.144	0.001*
≤ 20	280	117 (21.3)	163 (29.7)		
> 20	818	432 (78.7)	386 (70.3)		
Lymph node metastasis				3.901	0.048*
Yes	560	297 (54.8)	263 (48.8)		
No	521	245 (45.2)	276 (51.2)		
Disease stage (AJCC7)				0.007	0.932
I + II	814	409 (74.6)	405 (74.9)		
III + IV	275	139 (25.4)	136 (25.1)		
Distant metastasis				1.676	0.195
Yes	22	8 (1.7)	14 (3)		
No	914	460 (98.3)	454 (97)		

Values are presented as number (%).

DONSON = downstream neighbor of son; TCGA = The Cancer Genome Atlas; AJCC7 = American Joint Committee on Cancer 7th Edition.

* p -value < 0.05.

Association of DONSON expression and clinicopathological features

The correlation between DONSON expression and clinicopathological features was analyzed to determine whether the DONSON expression level affects tumorigenesis in patients with BC. TCGA cohorts were divided into groups with low and high DONSON expression based on the median DONSON expression level. High DONSON expression was correlated with tumor size ($p = 0.001$) and LNM ($p = 0.048$) in TCGA cohort (**Table 1**). Overall, DONSON expression is probably correlated with LNM, thereby affecting tumor size.

DONSON knockdown suppresses tumor proliferation *in vitro*

Specific siRNAs were used to knock down DONSON expression in BC cells for further experiments. The mRNA expression in the cell lines was generally reduced to a value < 0.25 (Figure. 2A), and DONSON protein levels were significantly downregulated (Figure. 2B). These results suggest that siRNAs reduce the expression of DONSON. Then, CCK-8 and colony formation assays were performed to evaluate the effect of DONSON on BC cell growth and explore its potential biological functions. DONSON knockdown significantly impaired MDA-MB-231 and BT-549 cell proliferation (**Figure 2C and D**). Furthermore, EdU incorporation assay was performed and showed that DONSON knockdown reduced the fluorescence intensity (**Figure 2E**), suppressing tumor proliferation *in vitro*.

DONSON knockdown induces apoptosis *in vitro*

Flow cytometry was used to measure the apoptosis of transfected MDA-MB-231 and BT-549 cells and elucidate the effect of DONSON on apoptosis. Apoptotic cells were positively stained for annexin V alone or both annexin V and PI. PI cannot stain live cells but can easily stain dead cells. Based on these results, DONSON-silenced BC cells exhibited an increased apoptosis rate compared to the control cells (**Figure 3A**). The bar graph shows the percentages of late and early apoptotic cells in each line (MDA-MB-231: si-NC 7.69 ± 1.117 , siRNA1 18.295 ± 2.977 , siRNA2 18.820 ± 1.994 ; BT-549: si-NC 2.195 ± 1.095 , siRNA1 13.355 ± 0.495 , siRNA2 14.985 ± 1.275) (**Figure 3B**). Caspase-3 is essential for certain processes associated with the dismantling of the cell and formation of apoptotic bodies and may also function before or at the stage of commitment to loss of cell viability [14]. DONSON

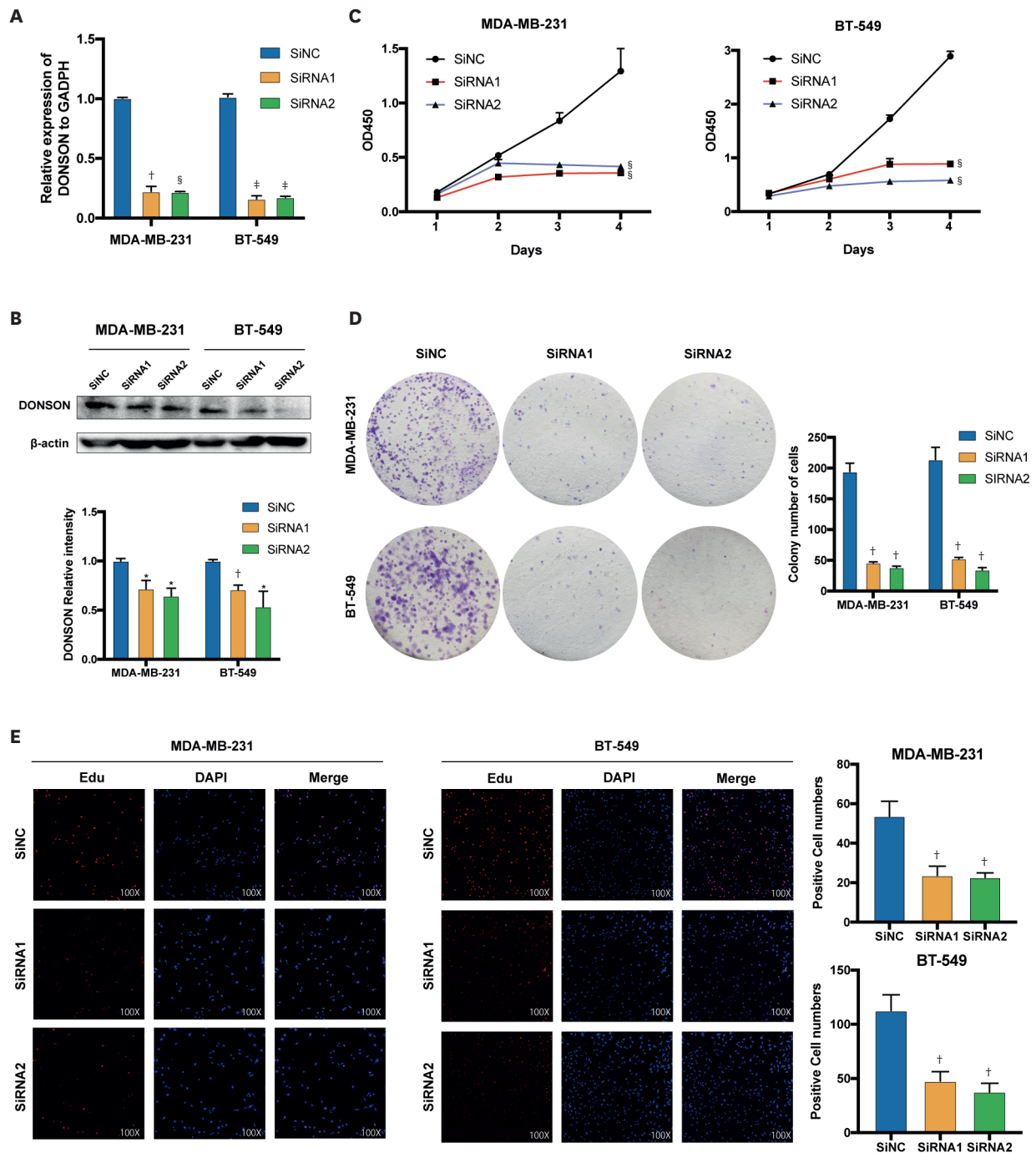


Figure 2. Effect of DONSON on the proliferation of BC cell lines. (A) The efficiency of siRNAs in BC cell lines was measured by qRT-PCR. (B) Levels of DONSON protein in BT-549 and MDA-MB-231 cells were measured by Western blot analysis. (C) Proliferation rates of control and DONSON knockdown MDA-MB-231 and BT-549 cells by the CCK-8 assay. (D) Representative images of colonies formed by MDA-MB-231 and BT-549 cells following DONSON knockdown. (E) Proliferation of MDA-MB-231 and BT-549 cells was detected using BeyoClick™ Edu-555 (red) immunofluorescence staining kit. The $2^{-\Delta\Delta Ct}$ method was used to represent the fold variation in expression detected using qRT-PCR. The images shown are representative of 3 independent experiments. DONSON = downstream neighbor of son; BC = breast cancer; qRT-PCR = quantitative reverse transcription polymerase chain reaction; CCK-8 = Cell Counting Kit-8; GAPDH = glyceraldehyde-3-phosphate dehydrogenase; OD = optical density; DAPI = 4',6-diamidino-2-phenylindole. * $p < 0.05$, [†] $p < 0.01$, [‡] $p < 0.001$, and [§] $p < 0.0001$ compared with the control group using Student's *t*-test.

knockdown significantly increased the caspase-3 activity (Figure 3C). Overall, DONSON knockdown markedly promoted apoptosis *in vitro*.

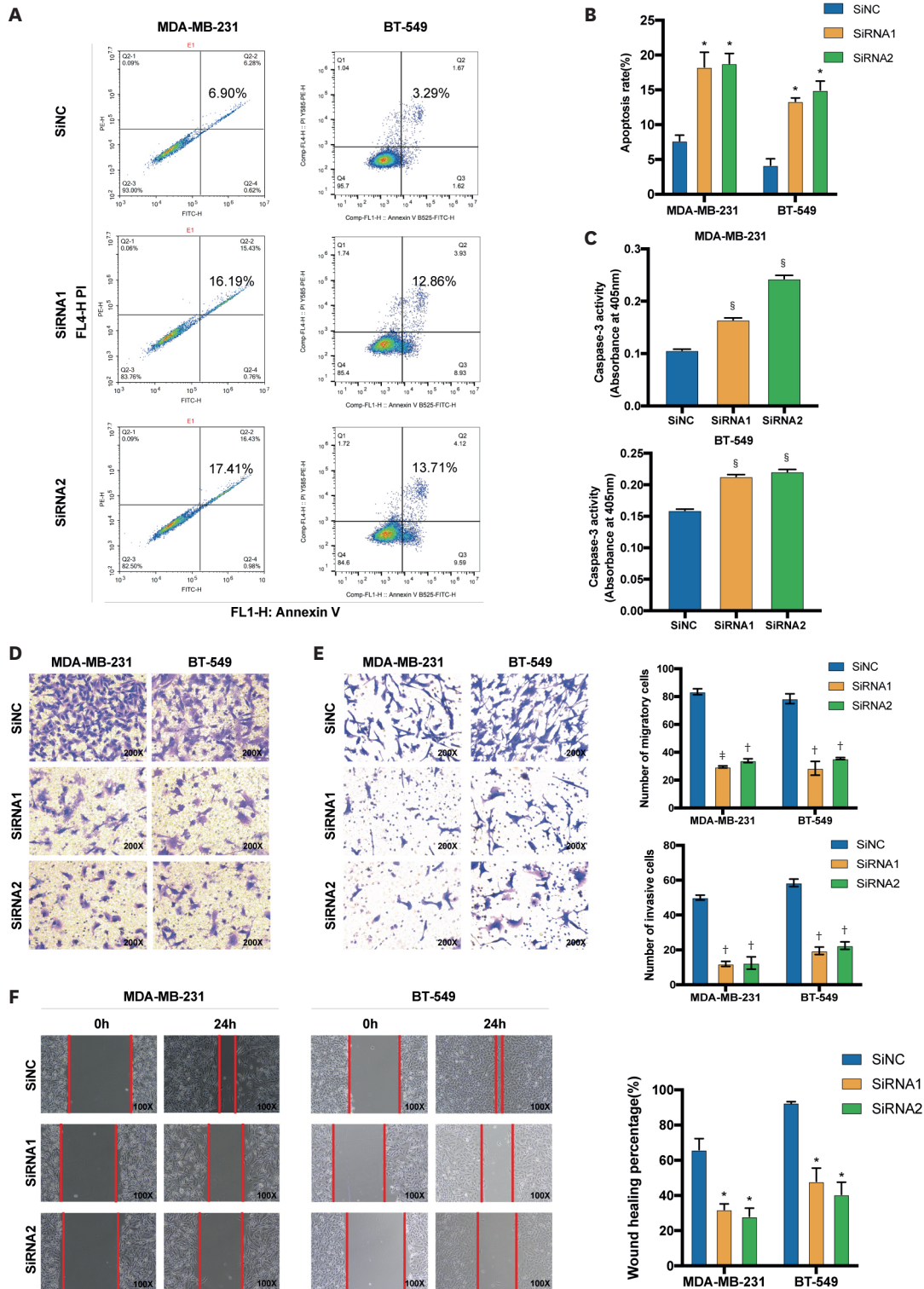


Figure 3. DONSON knockdown promotes the cell apoptosis and suppresses the migration and invasion of BC cell lines. (A, B) Percentage of apoptotic cells in the control and DONSON knockdown MDA-MB-231 and BT-549 cells. (C) Caspase 3 activity was evaluated using a Caspase Assay Kit, and the absorbance was measured at 405 nm. (D, E) Representative images of the Transwell cell migration and invasion assay showing the migration and invasion rates of MDA-MB-231 and BT-549 cells after DONSON knockdown. (F) Representative images of the wound healing assay showing the migration of MDA-MB-231 and BT-549 cells after DONSON knockdown. Images shown are representative of 3 separate experiments.

DONSON = downstream neighbor of son; BC = breast cancer.

* $p < 0.05$, † $p < 0.01$, ‡ $p < 0.001$ and § $p < 0.0001$ compared with the control group using Student's *t*-test.

DONSON knockdown impedes migration and invasion *in vitro*

The ability of MDA-MB-231 and BT-549 cells to migrate and invade was evaluated by Transwell cell migration and Matrigel invasion assays to determine the possible biological functions of DONSON. Matrigel-coated Transwell plates were used to perform invasion assays, whereas uncoated Transwell plates were used to examine cell migration. According to the migration tests, DONSON silencing repressed cellular migration compared to that in the negative control BC cell line (**Figure 3D**). The numbers of migrating cells were as follows: MDA-MB-231: si-NC 83.5 ± 2.121 , siRNA1 29.5 ± 0.707 , siRNA2 34 ± 1.414 , and BT-549: si-NC 83 ± 8.185 , siRNA1 24 ± 8.544 , siRNA2 31 ± 7.81 . Moreover, according to the invasion tests, DONSON knockdown repressed cellular invasion compared to that in the si-NC group (**Figure 3E**). The numbers of invading cells were as follows: MDA-MB-231: si-NC 50 ± 1.414 , siRNA1 12 ± 1.414 , siRNA2 12.5 ± 3.563 ; BT-549: si-NC 58.5 ± 2.121 , siRNA1 20.5 ± 0.707 , siRNA2 22.5 ± 2.121 . The scratch tests showed similar results. With silenced DONSON, the gaps between cells were significantly more extensive in BC cell lines (**Figure 3F**). Based on these results, DONSON knockdown significantly inhibited the migration and invasion of BC cells *in vitro*.

Overexpression of DONSON promoted the proliferation of BC cells and inhibits apoptosis

To verify that DONSON is an oncogene in BC, DONSON low HS-578T cells were transfected with the overexpression plasmid (**Figure 1I**), which increased DONSON levels compared to cells transfected with the pCMV vector (**Figure 4A and B**). As expected, the overexpression of DONSON markedly increased the proliferation (**Figure 4C-E**) and migration (**Figure 4F and G**) of HS-578T cells and decreased apoptosis rates (**Figure 4H**). Therefore, DONSON functions as an oncogene in BC, promoting proliferation and migration and inhibiting apoptosis.

DONSON knockdown decreases the number of cells at the S/G2 transition *in vitro*

GO terms, KEGG pathway, and functional enrichment analyses were performed using GSEA to investigate other potential biological functions of DONSON. As shown in **Figure 5A**, the cell cycle was enriched in the KEGG pathways (false discovery rate [FDR] < 0.001 , normalized enrichment score = 2.46) and GO terms (FDR < 0.001 , normalized enrichment score = 2.99). CDK2 drives cell progression into the S and M phases of the cell cycle [15]. The DONSON expression was significantly positively correlated with CDK2 expression in TIMER (**Figure 5B**, $\text{cor} = 0.589$, $p < 0.01$). Therefore, flow cytometry was used to analyze the cell cycle of transfected MDA-MB-231 and BT-549 cells. Furthermore, cells were serum-starved before transfection to synchronize the cell cycle. DONSON knockdown delayed S/G2 transition. Furthermore, the histograms show the statistical significance of the changes in the cell cycle in this experiment (**Figure 5C**). Then, according to Western blot analysis, DONSON knockdown significantly reduced the cyclin A1 and CDK2 levels (**Figure 5D**). Thus, DONSON blocked the cell cycle in the S phase of BC cells.

DONSON induces the epithelial-mesenchymal transition (EMT) in BC cell lines

EMT is a crucial characteristic of tumorigenesis [16]. Therefore, the levels of EMT-related proteins were quantified as representative markers in BC cells. E-cadherin is an epithelial marker that suppresses tumor invasion [17,18] and N-cadherin is a mesenchymal marker of EMT and cancer metastasis [19]. Switching between these markers (E-cadherin to N-cadherin) is a critical hallmark of EMT [20]. DONSON knockdown increased the levels of the epithelial marker (E-cadherin) and decreased the levels of several mesenchymal markers, including N-cadherin. Furthermore, as a cytoskeletal protein, vimentin filaments support the mechanical integrity of the migratory machinery, generation of directional force,

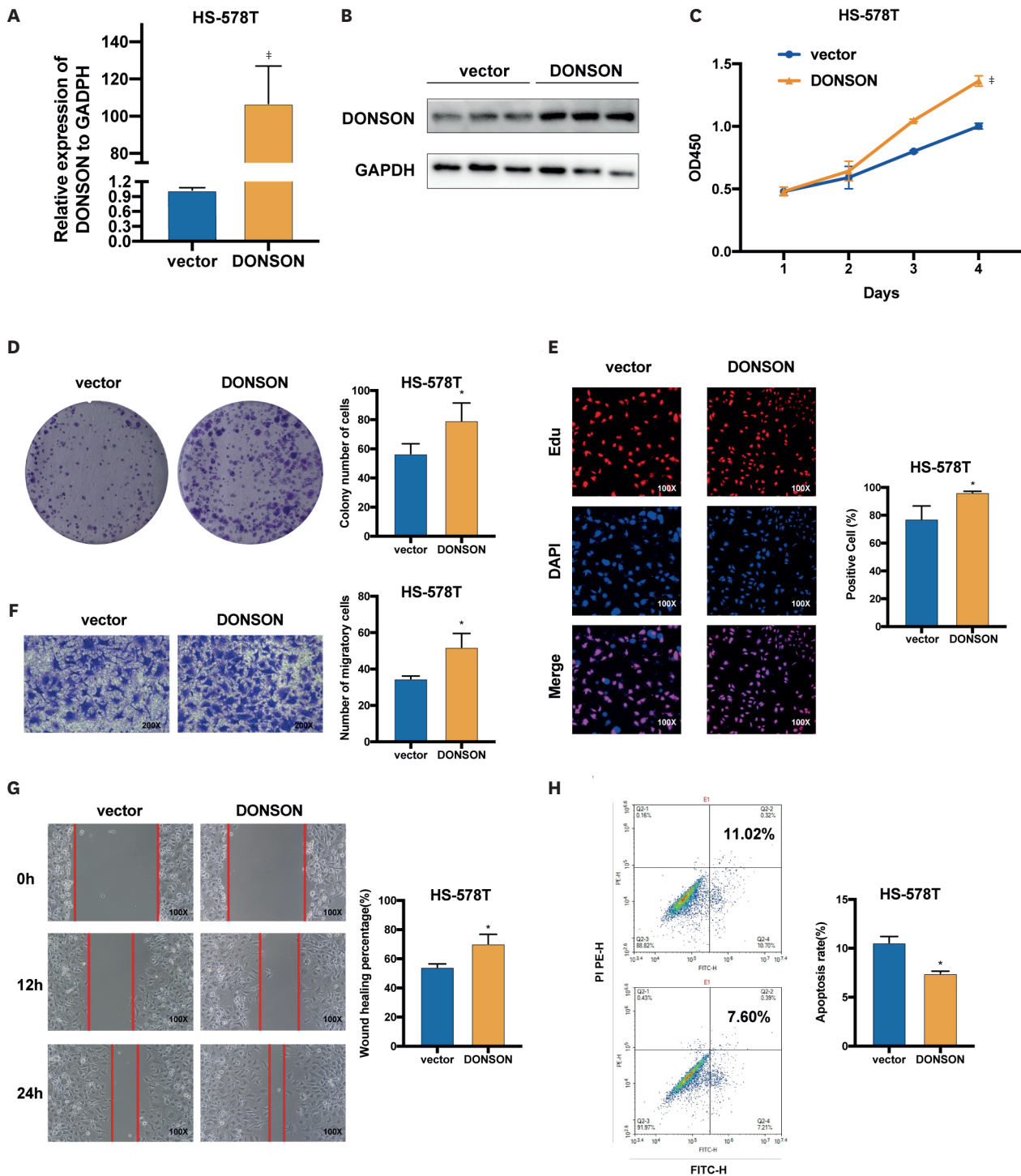


Figure 4. Overexpression of DONSON promotes the proliferation of BC cells and inhibits apoptosis. (A, B) DONSON expression levels in HS-578T cells transfected with pCMV and pCMV-DONSON. (C) Proliferation rates of control and DONSON-overexpressing HS-578T cells. (D) Representative images of colonies formed by control and DONSON-overexpressing HS-578T cells. (E) Edu incorporation in the indicated groups. (F) Representative images of the Transwell migration assay showing the migration rates of control and DONSON-overexpressing HS-578T cells. (G) Representative images showing the extent of wound by the DONSON-overexpressing HS-578T cells. (H) Percentage of apoptotic cells in the indicated groups. Images shown are representative of 3 separate experiments. DONSON = downstream neighbor of son; BC = breast cancer; GAPDH = glyceraldehyde-3-phosphate dehydrogenase. * $p < 0.05$ and $^{\ddagger}p < 0.001$ compared with the control using Student's *t*-test.

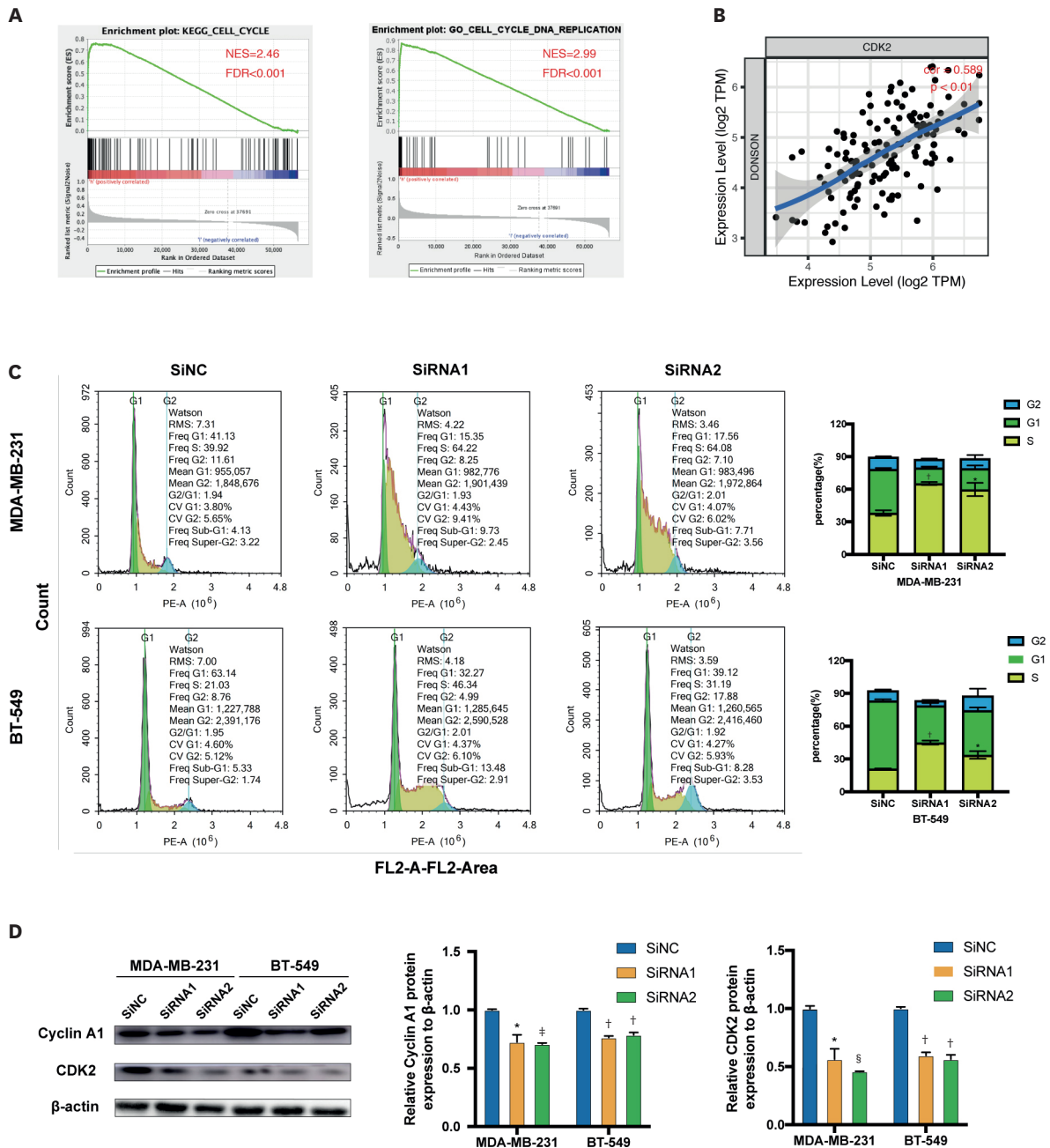


Figure 5. DONSON knockdown blocks the cell cycle at the S/G2 transition in BC cell lines. (A) A single GSEA using TCGA data investigated the potential biological functions of DONSON. (B) The correlation between DONSON and CDK2 was analyzed using TIMER. (C) Flow cytometry plots showing the cell cycle distribution in the indicated groups. (D) Representative immunoblots showing the expression levels of cyclin A1 and CDK2 after DONSON knockdown. The images shown are representative of 3 independent experiments.

DONSON = downstream neighbor of son; BC = breast cancer; GSEA = gene set enrichment analysis; TCGA = The Cancer Genome Atlas; CDK2 = cyclin-dependent kinase 2; TIMER = Tumor IMMune Estimation Resource; NES = normalized enrichment score; FDR = false discovery rate.

* $p < 0.05$, † $p < 0.01$, ‡ $p < 0.001$, and § $p < 0.0001$ compared with the control using Student's *t*-test.

focal adhesion modulation, and extracellular attachment [21]. DONSON knockdown also decreased the vimentin levels.

The Bcl-2 gene family, which is involved in the cellular mitochondrial apoptosis pathway, consists of pro-apoptotic (Bax) and anti-apoptotic (Bcl-2) genes [22]. In this study, DONSON

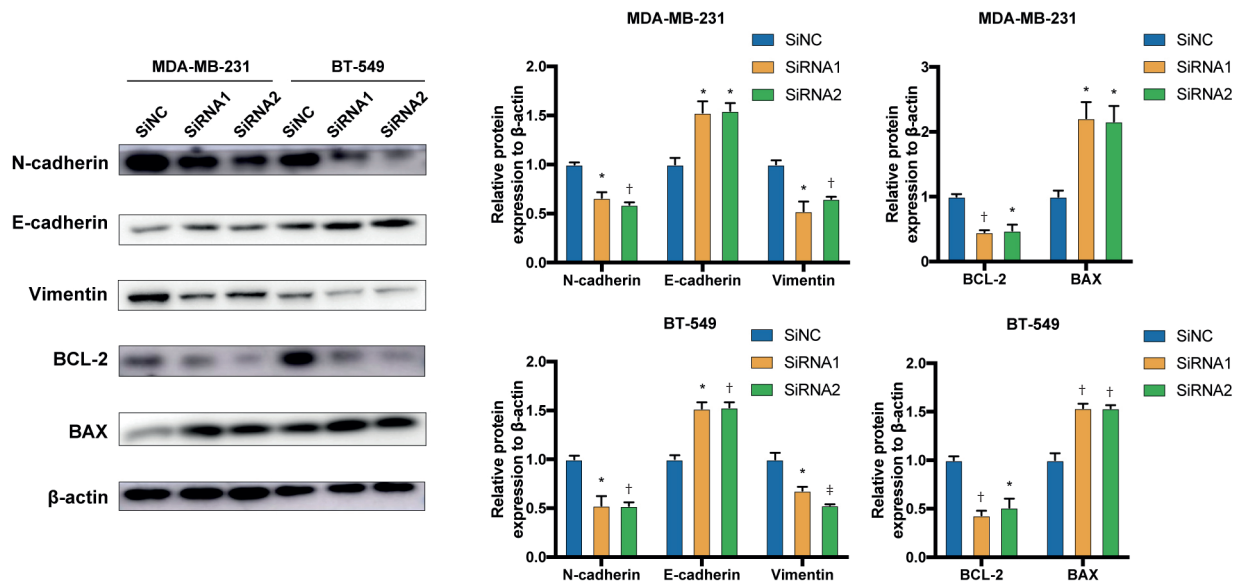


Figure 6. DONSON alters the expression of proteins related to apoptosis and the EMT. Representative immunoblots showing the expression levels of the Bax, Bcl-2, E-cadherin, N-cadherin, and vimentin proteins after DONSON knockdown. Images shown are representative of 3 separate experiments.

DONSON = downstream neighbor of son; EMT = epithelial-mesenchymal transition.

* $P < 0.05$, † $P < 0.01$, and ‡ $P < 0.001$ compared with the control using Student's *t*-test.

knockdown increased Bax and decreased Bcl-2 expression (Figure 6). These results demonstrated that DONSON promotes EMT and hinders apoptosis in BC cells.

DISCUSSION

Heterogeneous evolution and genetic changes complicate BC treatment [23]. Therefore, studies exploring new molecular markers that predict the prognosis of the disease and improve our understanding of the disease mechanism will be helpful for precise treatment. According to our RNA sequencing results, DONSON is one of the genes with significantly elevated expression in BC. DONSON expression is also increased in other tumors. According to previous studies, DONSON is correlated with the prognosis of patients with RCC [7]. Nevertheless, the specific function of DONSON in BC remains unclear.

This study verified that DONSON is expressed at high levels in BC samples available in public databases and then confirmed DONSON expression within the validation cohort and BC cell line using qRT-PCR. Meanwhile, high expression of DONSON was correlated with poor prognosis of patients in public databases. Then, the correlation between DONSON expression and clinical characteristics using TCGA data was investigated, and the results revealed that DONSON expression may be related to LNM and tumor size. According to a loss-of-function experiment, DONSON promotes proliferation, migration, invasion, and S/G2 transition of BC cells *in vitro*. DONSON also hinders apoptosis of BC cells *in vitro*. EMT is a vital process that affects tumor heterogeneity and triggers a spectrum of tumor cell phenotypes with the ability to promote tumor progression through various mechanisms [19,24]. Apoptosis is a hallmark of most cancers [25]. Certain proteins involved in EMT are thought to promote tumor cell survival by suppressing apoptosis [26]. Moreover, Bcl-2, a protein that protects against apoptosis, induces EMT [27]. Therefore, the crosstalk between EMT and apoptosis represents a crucial cellular process involved in tumor metastasis and

invasion. The protein levels of EMT-related and apoptosis-related genes were examined, and DONSON knockdown increased the expression of E-cadherin and Bax and decreased the expression of N-cadherin, vimentin, and Bcl-2 in BC cell lines compared with those in control cells. Based on these results, DONSON is likely to facilitate EMT and reduce apoptosis in BC cells. Conversely, CDKs are protein kinases capable of regulating the cell cycle in tumor cells and affect tumor growth [28]. Recently, CDK inhibitors have been considered for tumor treatment [29]. It was found that DONSON knockdown also reduced the expression of cyclin A1 and CDK2. These results confirm that DONSON is an oncogene in BC that may promote proliferation by regulating CDKs. Therefore, it may be a potential therapeutic target for BC treatment. CDK inhibitors interfere with CDK function during tumor treatment. Therefore, CDK inhibitors combined with DONSON knockout may represent a new treatment strategy for BC. Currently, clustered regularly interspaced short palindromic repeats (CRISPRs) serve as a guide for the endonuclease Cas9 (CRISPR-associated protein 9) to recognize and cleave specific strands of DNA that are complementary to the CRISPR sequence. CRISPR/Cas9-mediated editing is a technology for specific DNA modification of targeted genes, and is fast, robust, and efficient [30,31]. We can use CRISPR/Cas9 technology to selectively knock down DONSON in patients with BC, thus inhibiting the progression of BC. Moreover, antisense oligonucleotides (ASOs) are used to selectively inhibit the translation of disease-associated genes via ribonuclease H-mediated cleavage or steric hindrance. They have been developed as a novel and promising class of drugs that target a wide range of diseases [32]. We can design ASO drugs targeting DONSON for BC treatment.

Nevertheless, our study has some limitations. First, further studies are needed to determine whether DONSON directly alters CDK2 and cyclin A1 expression or indirectly through other proteins. Second, the level of DONSON protein in BC tissues requires validation. Third, the function of DONSON in BC must be further verified *in vivo*.

Overall, DONSON is highly expressed in BC tissues and cell lines. Moreover, according to the clinicopathological analysis, LNM and tumor size are 2 of the critical features correlated with DONSON expression. The results revealed the biological function and possible mechanism of action of DONSON in BC. Our experiments showed that DONSON may promote BC development by regulating EMT and CDKs. Based on these results, DONSON functions as an oncogene and is likely to represent a possible therapeutic target for BC.

ACKNOWLEDGMENTS

The authors appreciate all doctors of the Department of Thyroid and Breast Surgery, The First Affiliated Hospital of Wenzhou Medical University, for providing all essential data.

REFERENCES

1. Siegel RL, Miller KD, Jemal A. Cancer statistics, 2020. *CA Cancer J Clin* 2020;70:7-30.
[PUBMED](#) | [CROSSREF](#)
2. Howlader N, Altekruse SF, Li CI, Chen VW, Clarke CA, Ries LA, et al. US incidence of breast cancer subtypes defined by joint hormone receptor and HER2 status. *J Natl Cancer Inst* 2014;106:dju055.
[PUBMED](#) | [CROSSREF](#)
3. Prat A, Saura C, Pascual T, Hernando C, Muñoz M, Paré L, et al. Ribociclib plus letrozole versus chemotherapy for postmenopausal women with hormone receptor-positive, HER2-negative, luminal

- B breast cancer (CORALLEEN): an open-label, multicentre, randomised, phase 2 trial. *Lancet Oncol* 2020;21:33-43.
[PUBMED](#) | [CROSSREF](#)
4. von Minckwitz G, Procter M, de Azambuja E, Zardavas D, Benyunes M, Viale G, et al. Adjuvant pertuzumab and trastuzumab in early HER2-positive breast cancer. *N Engl J Med* 2017;377:122-31.
[PUBMED](#) | [CROSSREF](#)
 5. DeSantis CE, Ma J, Gaudet MM, Newman LA, Miller KD, Goding Sauer A, et al. Breast cancer statistics, 2019. *CA Cancer J Clin* 2019;69:438-51.
[PUBMED](#) | [CROSSREF](#)
 6. Lim B, Hortobagyi GN. Current challenges of metastatic breast cancer. *Cancer Metastasis Rev* 2016;35:495-514.
[PUBMED](#) | [CROSSREF](#)
 7. Klümper N, Blajan I, Schmidt D, Kristiansen G, Toma M, Hölzel M, et al. Downstream neighbor of SON (DONSON) is associated with unfavorable survival across diverse cancers with oncogenic properties in clear cell renal cell carcinoma. *Transl Oncol* 2020;13:100844.
[PUBMED](#) | [CROSSREF](#)
 8. Klümper N, von Danwitz M, Stein J, Schmidt D, Schmidt A, Kristiansen G, et al. Downstream neighbor of son (DONSON) expression is enhanced in phenotypically aggressive prostate cancers. *Cancers (Basel)* 2020;12:3439.
[PUBMED](#) | [CROSSREF](#)
 9. Tang Z, Li C, Kang B, Gao G, Li C, Zhang Z. GEPIA: a web server for cancer and normal gene expression profiling and interactive analyses. *Nucleic Acids Res* 2017;45:W98-102.
[PUBMED](#) | [CROSSREF](#)
 10. Mootha VK, Lindgren CM, Eriksson KF, Subramanian A, Sihag S, Lehar J, et al. PGC-1alpha-responsive genes involved in oxidative phosphorylation are coordinately downregulated in human diabetes. *Nat Genet* 2003;34:267-73.
[PUBMED](#) | [CROSSREF](#)
 11. Li T, Fan J, Wang B, Traugh N, Chen Q, Liu JS, et al. TIMER: a web server for comprehensive analysis of tumor-infiltrating immune cells. *Cancer Res* 2017;77:e108-10.
[PUBMED](#) | [CROSSREF](#)
 12. Germain DR, Graham K, Glubrecht DD, Hugh JC, Mackey JR, Godbout R. DEAD box 1: a novel and independent prognostic marker for early recurrence in breast cancer. *Breast Cancer Res Treat* 2011;127:53-63.
[PUBMED](#) | [CROSSREF](#)
 13. Komatsu M, Yoshimaru T, Matsuo T, Kiyotani K, Miyoshi Y, Tanahashi T, et al. Molecular features of triple negative breast cancer cells by genome-wide gene expression profiling analysis. *Int J Oncol* 2013;42:478-506.
[PUBMED](#) | [CROSSREF](#)
 14. Porter AG, Jänicke RU. Emerging roles of caspase-3 in apoptosis. *Cell Death Differ* 1999;6:99-104.
[PUBMED](#) | [CROSSREF](#)
 15. Tadesse S, Caldon EC, Tilley W, Wang S. Cyclin-dependent kinase 2 inhibitors in cancer therapy: an update. *J Med Chem* 2019;62:4233-51.
[PUBMED](#) | [CROSSREF](#)
 16. Richards EJ, Zhang G, Li ZP, Permeth-Wey J, Challa S, Li Y, et al. Long non-coding RNAs (LncRNA) regulated by transforming growth factor (TGF) β : LncRNA-hit-mediated TGF β -induced epithelial to mesenchymal transition in mammary epithelia. *J Biol Chem* 2015;290:6857-67.
[PUBMED](#) | [CROSSREF](#)
 17. Meigs TE, Fedor-Chaikin M, Kaplan DD, Brackenbury R, Casey PJ. Galpha12 and Galpha13 negatively regulate the adhesive functions of cadherin. *J Biol Chem* 2002;277:24594-600.
[PUBMED](#) | [CROSSREF](#)
 18. Grete S, Howe PH. hnRNP E1 at the crossroads of translational regulation of epithelial-mesenchymal transition. *J Cancer Metastasis Treat* 2019;5:16.
[PUBMED](#) | [CROSSREF](#)
 19. Nieto MA, Huang RY, Jackson RA, Thiery JP. EMT: 2016. *Cell* 2016;166:21-45.
[PUBMED](#) | [CROSSREF](#)
 20. Wheelock MJ, Shintani Y, Maeda M, Fukumoto Y, Johnson KR. Cadherin switching. *J Cell Sci* 2008;121:727-35.
[PUBMED](#) | [CROSSREF](#)
 21. Usman S, Waseem NH, Nguyen TK, Mohsin S, Jamal A, Teh MT, et al. Vimentin is at the heart of epithelial mesenchymal transition (EMT) mediated metastasis. *Cancers (Basel)* 2021;13:4985.
[PUBMED](#) | [CROSSREF](#)

22. Renault TT, Dejean LM, Manon S. A brewing understanding of the regulation of Bax function by Bcl-xL and Bcl-2. *Mech Ageing Dev* 2017;161:201-10.
[PUBMED](#) | [CROSSREF](#)
23. Testa U, Castelli G, Pelosi E. Breast cancer: a molecularly heterogenous disease needing subtype-specific treatments. *Med Sci (Basel)* 2020;8:18.
[PUBMED](#) | [CROSSREF](#)
24. Zeisberg M, Neilson EG. Biomarkers for epithelial-mesenchymal transitions. *J Clin Invest* 2009;119:1429-37.
[PUBMED](#) | [CROSSREF](#)
25. Hanahan D, Weinberg RA. The hallmarks of cancer. *Cell* 2000;100:57-70.
[PUBMED](#) | [CROSSREF](#)
26. Chakraborty S, Mir KB, Seligson ND, Nayak D, Kumar R, Goswami A. Integration of EMT and cellular survival instincts in reprogramming of programmed cell death to anastasis. *Cancer Metastasis Rev* 2020;39:553-66.
[PUBMED](#) | [CROSSREF](#)
27. Wu Y, Tang L. Bcl-2 family proteins regulate apoptosis and epithelial to mesenchymal transition by calcium signals. *Curr Pharm Des* 2016;22:4700-4.
[PUBMED](#) | [CROSSREF](#)
28. Malumbres M. Cyclin-dependent kinases. *Genome Biol* 2014;15:122.
[PUBMED](#) | [CROSSREF](#)
29. Heptinstall AB, Adiyasa I, Cano C, Hardcastle IR. Recent advances in CDK inhibitors for cancer therapy. *Future Med Chem* 2018;10:1369-88.
[PUBMED](#) | [CROSSREF](#)
30. Petazzi P, Menéndez P, Sevilla A. CRISPR/Cas9-mediated gene knockout and knockin human iPSCs. *Methods Mol Biol*. Epub 2020 Nov 15. https://doi.org/10.1007/7651_2020_337.
[PUBMED](#) | [CROSSREF](#)
31. Gupta D, Bhattacharjee O, Mandal D, Sen MK, Dey D, Dasgupta A, et al. CRISPR-Cas9 system: a new-fangled dawn in gene editing. *Life Sci* 2019;232:116636.
[PUBMED](#) | [CROSSREF](#)
32. Gagliardi M, Ashizawa AT. The challenges and strategies of antisense oligonucleotide drug delivery. *Biomedicines* 2021;9:433.
[PUBMED](#) | [CROSSREF](#)